Fig. S1

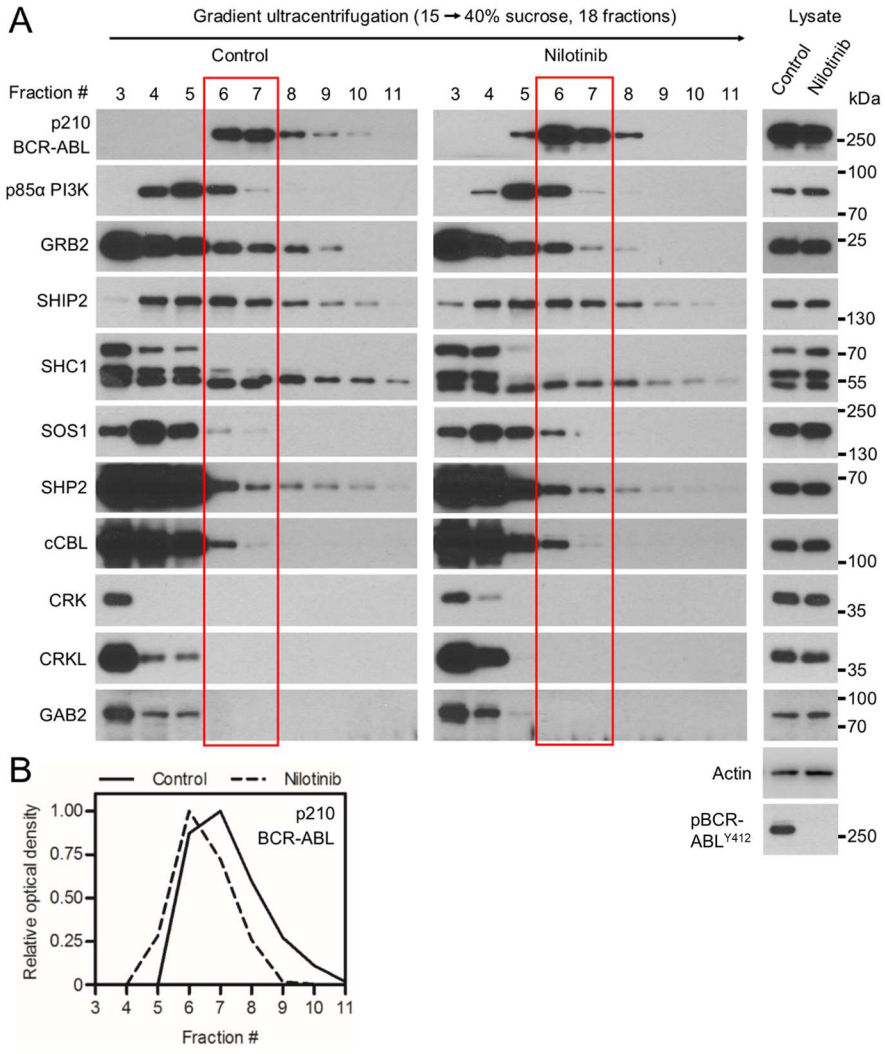


**Figure S1**

(A) 293T cells were transfected with p210 BCR-ABL, native cells lysates were subjected to ultracentrifugation in the 15-40% sucrose gradient, and the collected fractions were analyzed by western blot. Note the various degree of co-sedimentation of BCR-ABL with p85a-PI3K, GRB2, SHIP2, SHC1, SOS1, SHP2 and cCBL; no co-sedimentation with CRK, CRKL or GAB2 was seen. Inhibition of BCR-ABL kinase activity with 100 nM nilotinib resulted in a shift of a fraction of the BCR-ABL complexes towards lighter fractions, suggesting partial dissolution of the BCR-ABL signaling complex. (B) The western blot analysis of BCR-ABL was quantified as described in Material and Methods. Data show a single experiment out of three independent experiments carried-out. The fractions containing most of the p210 BCR-ABL are highlighted in red. Phosphorylation (p) at ABL Y412 was used to determine the degree of BCR-ABL inhibition using nilotinib; actin serves as a loading control in total cells lysates used for ultracentrifugation.

Fig. S2

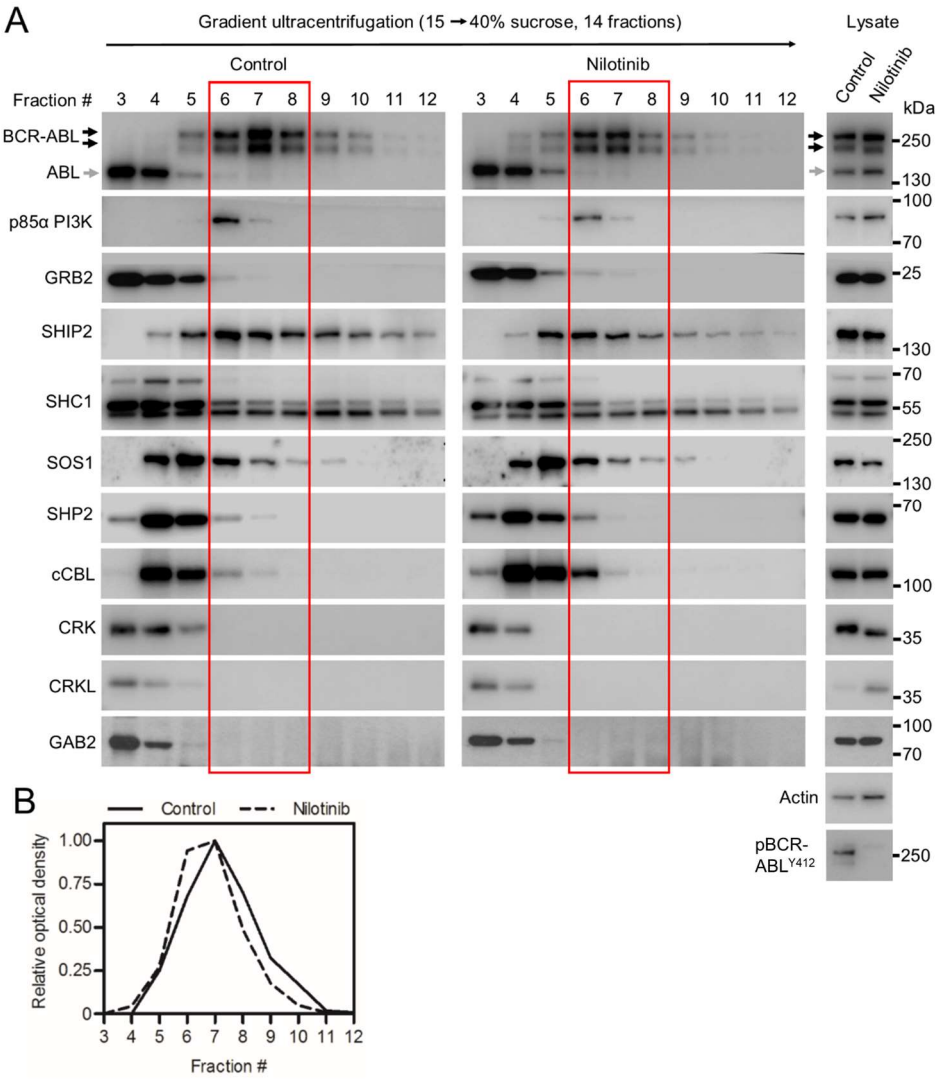


**Figure S2**

(A) K562 cell lysates were subjected to ultracentrifugation in the 15-40% sucrose gradient, and the collected fractions were analyzed by western blot. Note the various degree of co-sedimentation of BCR-ABL with p85a-PI3K, GRB2, SHIP2, SHC1, SOS1, SHP2 and cCBL; no co-sedimentation with CRK, CRKL or GAB2 was seen. Inhibition of BCR-ABL kinase activity with 1 μM nilotinib resulted in a shift of a fraction of the BCR-ABL complexes towards lighter fractions, suggesting partial dissolution of the BCR-ABL signaling complex. (B) The western blot analysis of BCR-ABL was quantified as described in Material and methods. Data show a single experiment out of three independent experiments carried-out. The fractions containing most of the p210 BCR-ABL are highlighted in red. Phosphorylation (p) at ABL Y412 was used to determine the degree of BCR-ABL inhibition using nilotinib; actin serves as a loading control in total cells lysates used for ultracentrifugation.

Fig. S3

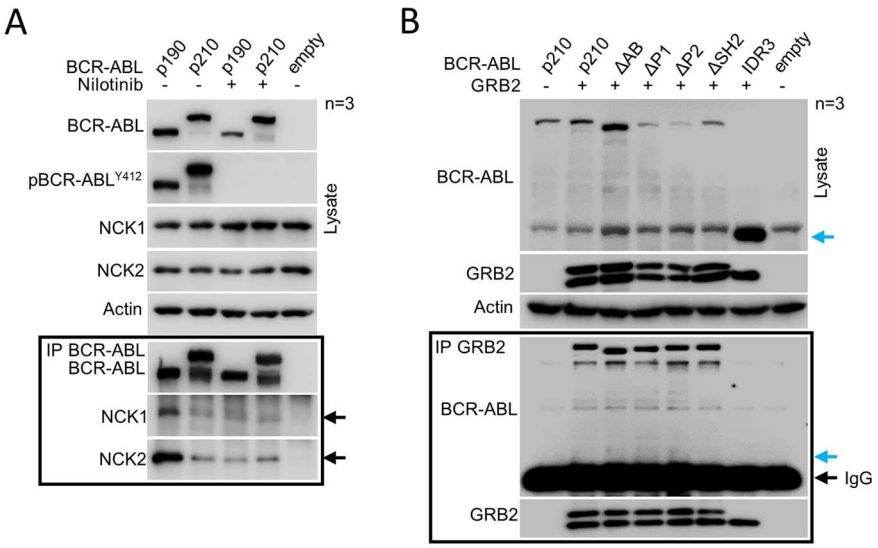


**Figure S3**
(A) NCK1 and NCK2 interact with BCR-ABL as well as nilotinib treated BCR-ABL. 293T cells were transfected by BCR-ABL construct and treated where indicated by 200nM nilotinib 1 hour post transfection. Cells were lysed and subjected to BCR-ABL FLAG IP, followed by western blot to detect NCK1 and NCK2 binding. Data are representative of three independent experiments, actin serves as a loading control. (B) GRB2 does not interact with IDR3 domain alone. 293T cells were cotransfected by BCR-ABL constructs and wt GRB2-V5. Cells were lysed and subjected to GRB2-V5 IP, followed by western blot to detect BCR-ABL binding. Blue arrows indicate position of the IDR3 construct, black arrow indicates IgG heavy from antibody used for IP. Data are representative of three independent experiments, actin serves as a loading control.

Fig. S4

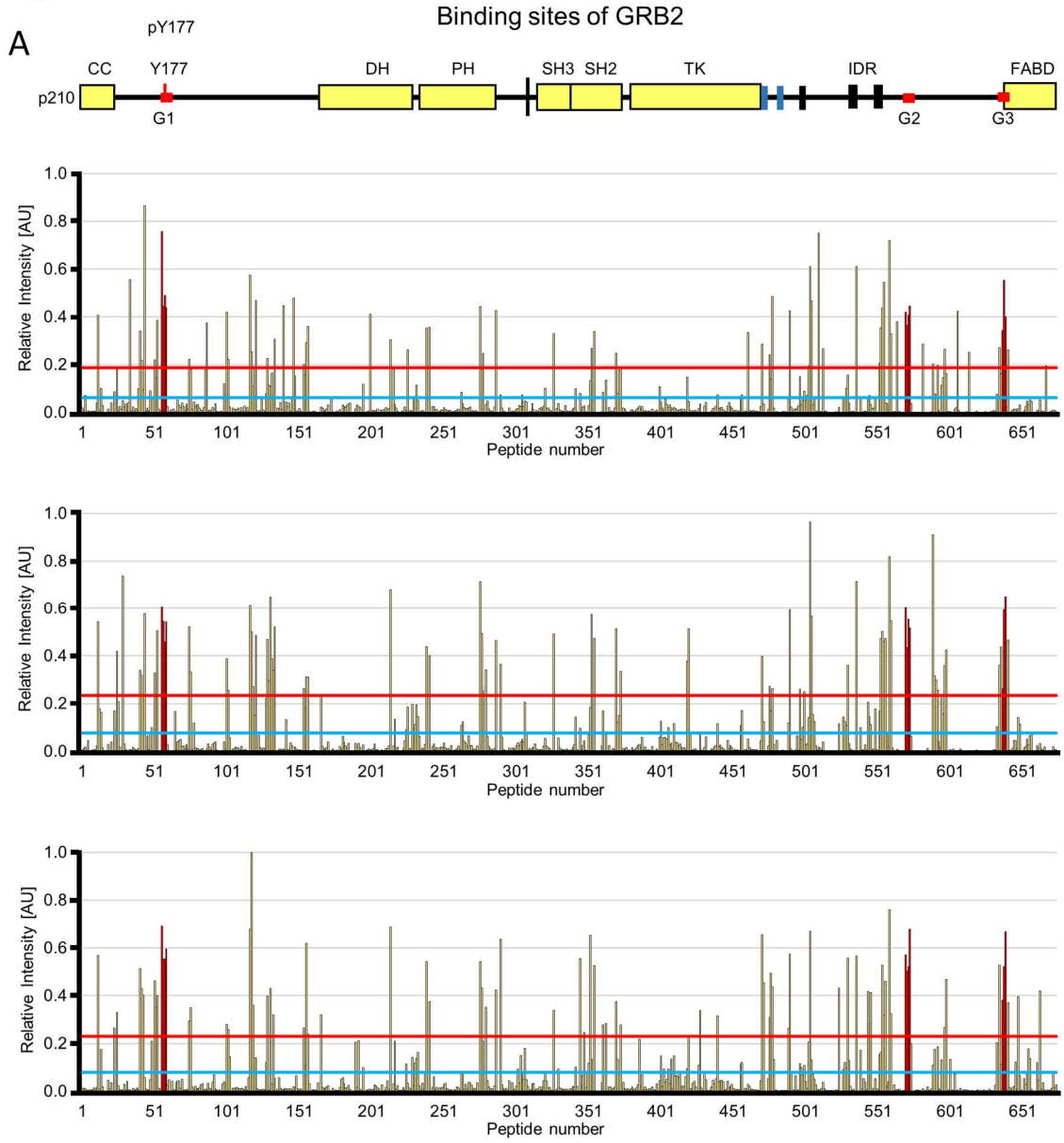
A
Binding sites of GRB2
pY177
CC
Y177
DH
PH
SH3
SH2
TK
IDR
FABD
p210
G1
G2
G3
Relative Intensity [AU]
Peptide number
B
CC
Y177
DH
PH
SH3
SH2
TK
IDR
FABD
g4
g5
g6
g7
g8
g9
Relative Intensity [AU]
Peptide number

**Figure S4**

(A) Microarray data for GRB2 binding to BCR-ABL. The three graphs represent technical replicates from which the values were averaged in main figures. Y axis shows relative fluorescent intensities for each peptide covering entire BCR-ABL sequence ordered from N to C terminus on X axis (peptide number). Blue lines represent average value from all peptides and red line indicates average + 1SD that is threshold, above which we considered signals to be positive. At least three consecutive peptides that exceeded the threshold in all three technical replicates are highlighted in red in graphs and as red bars in the BCR-ABL scheme above and form potential binding site. Sequences and phosphorylation status of respective binding sites are listed in supplementary tables S3 – S7. (B) Graph showing additional candidate GRB2 binding sites that did not meet our criteria of at least three consecutive peptides exceeding the threshold. Relative fluorescent intensity values were averaged from three technical replicates and plotted with SD. Red bars indicate above-threshold signals. Locations of these additional candidate sites is highlighted in blue in BCR-ABL scheme above.

Fig. S5

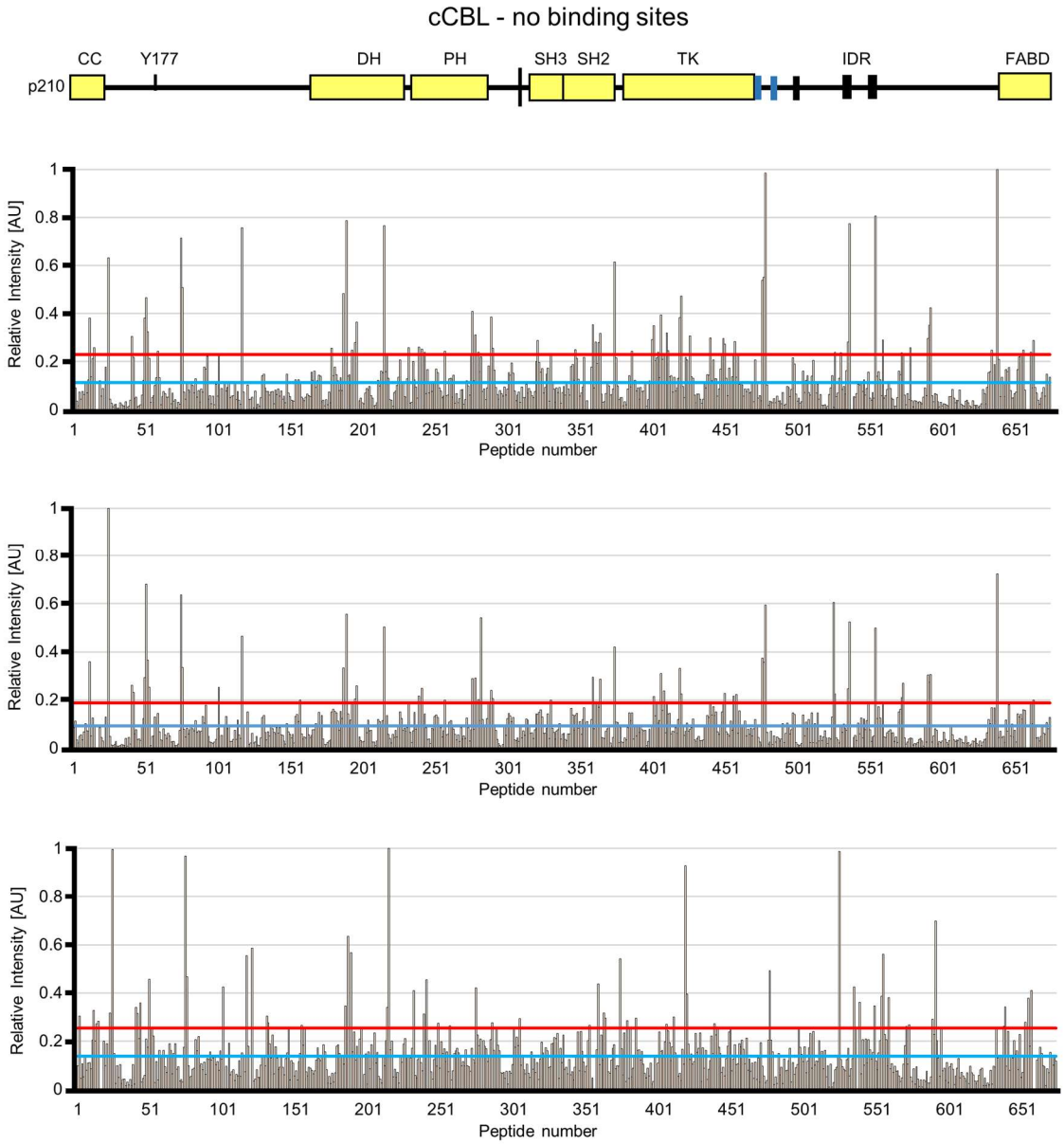


**Figure S5**
Microarray data for cCBL binding to BCR-ABL. No potential binding sites were detected.

Fig. S6

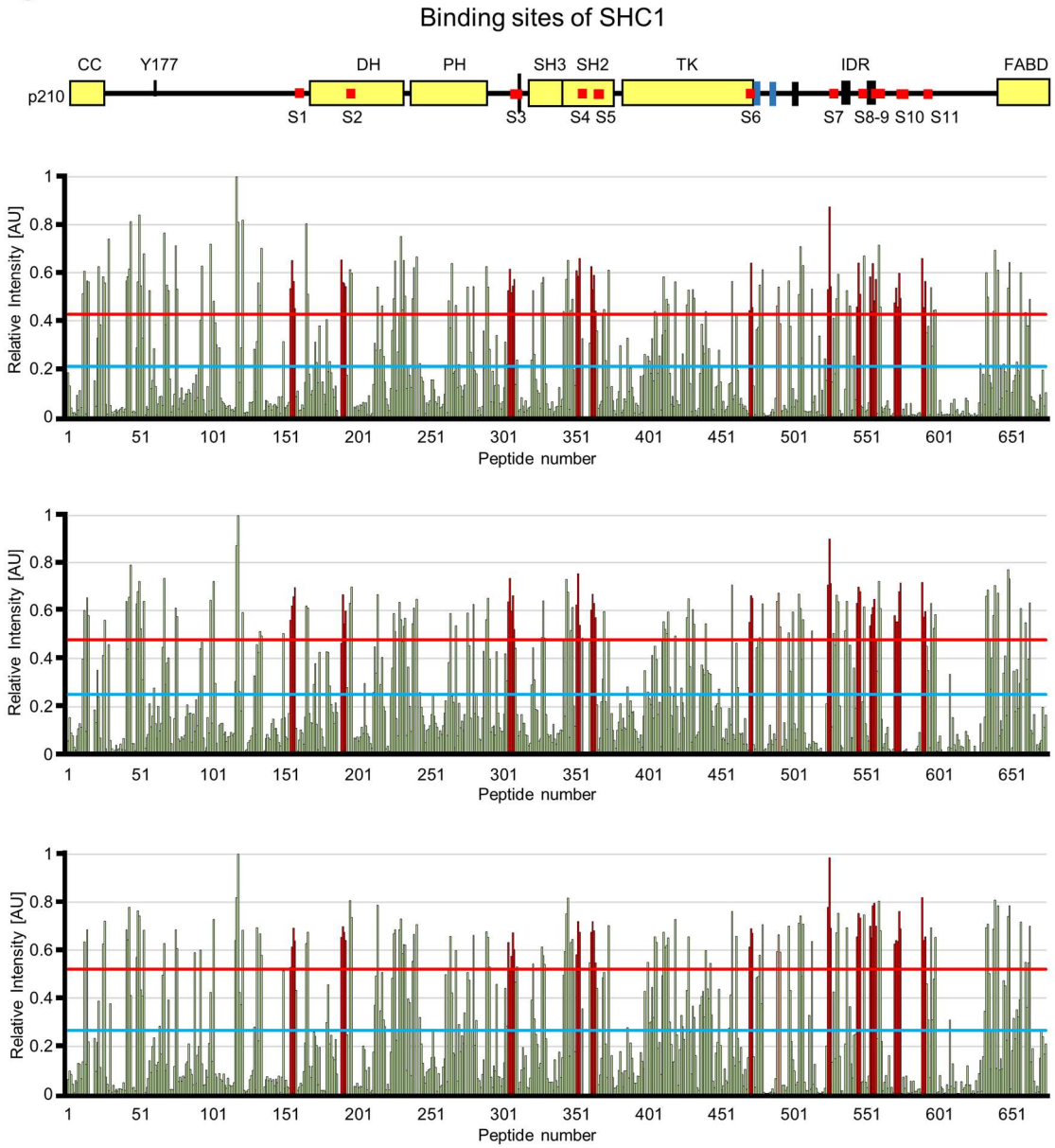


**Figure S6**
Microarray data for SHC1 binding to BCR-ABL.

Fig. S7

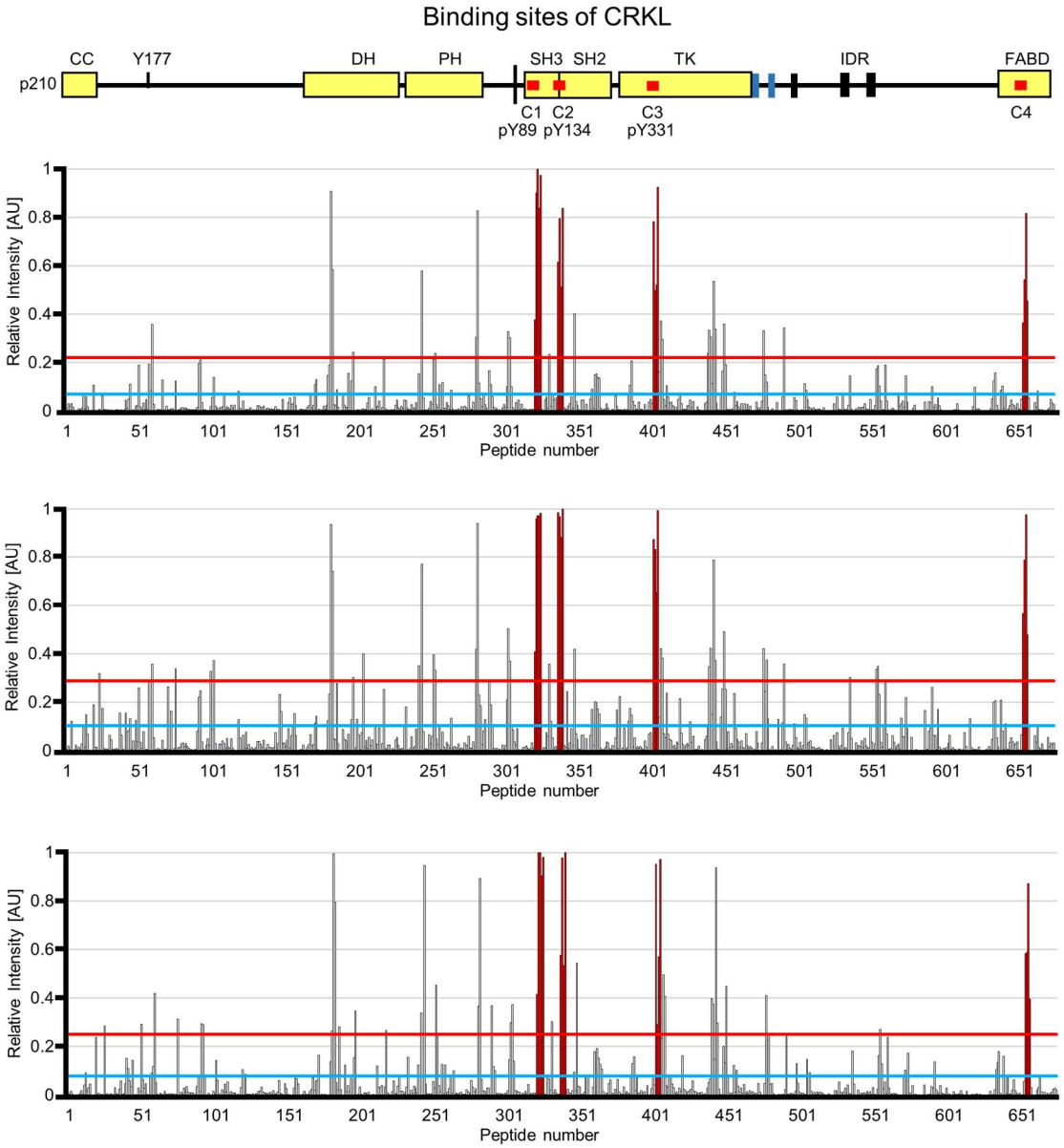


**Figure S7**
Microarray data for CRKL binding to BCR-ABL.

Fig. S8

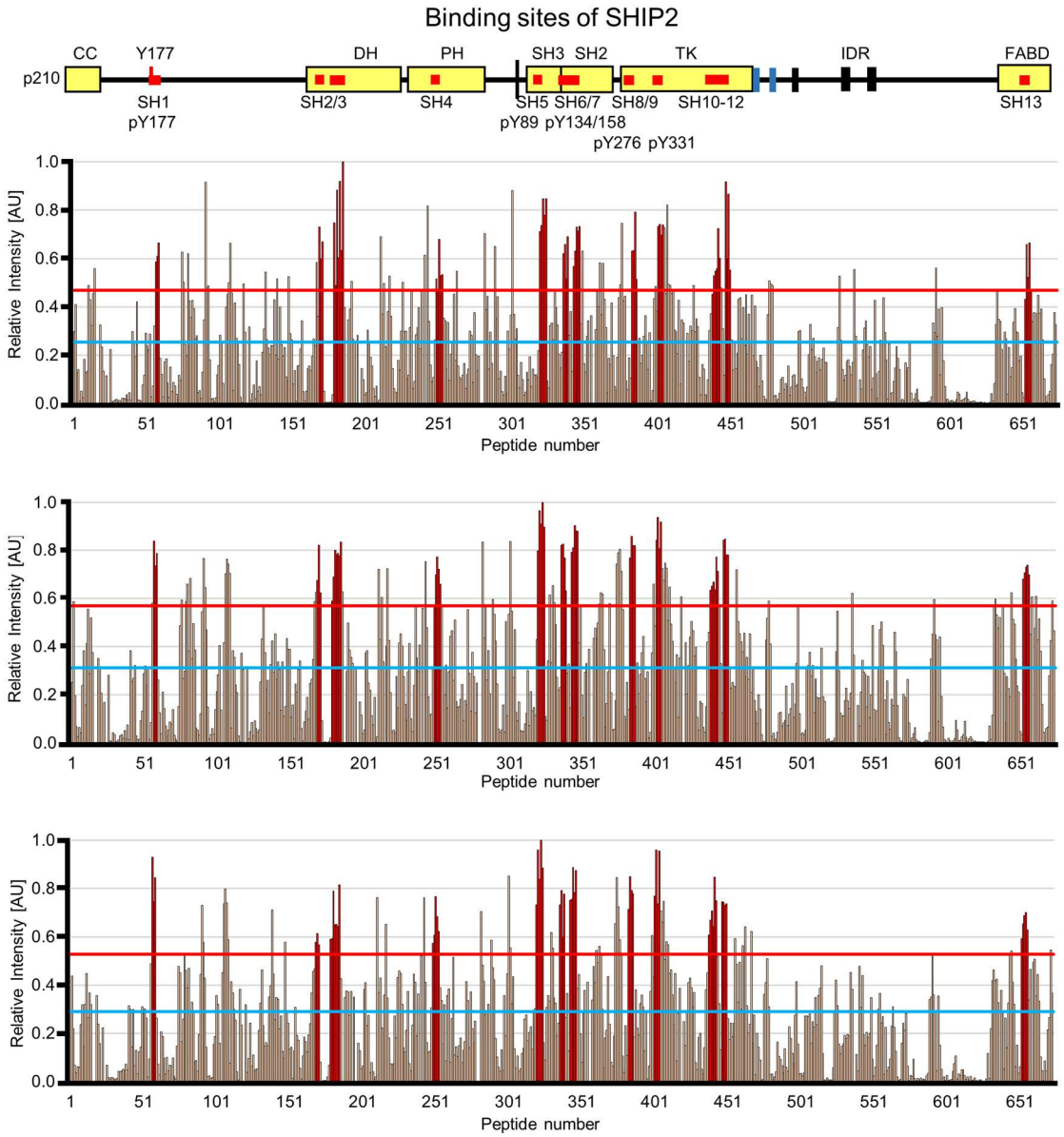


**Figure S8**
Microarray data for SHIP2 binding to BCR-ABL. SH12 binding site for Y488 is not highlighted in graphs, as it was found in independent experiment and is shown in Fig. 6D.

Fig. S9

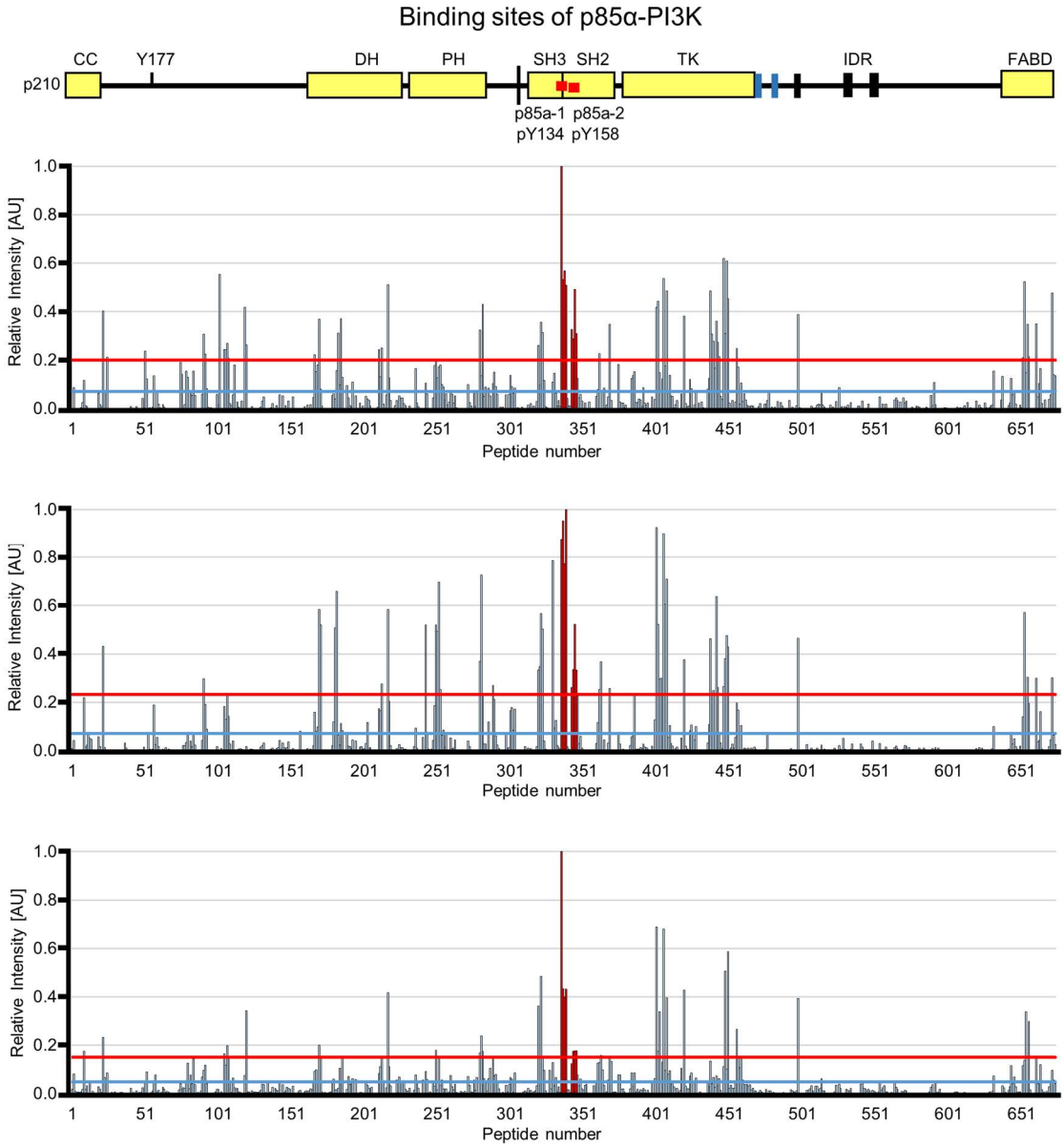


**Figure S9**
Microarray data for p85a-PI3K binding to BCR-ABL.

Fig. S10

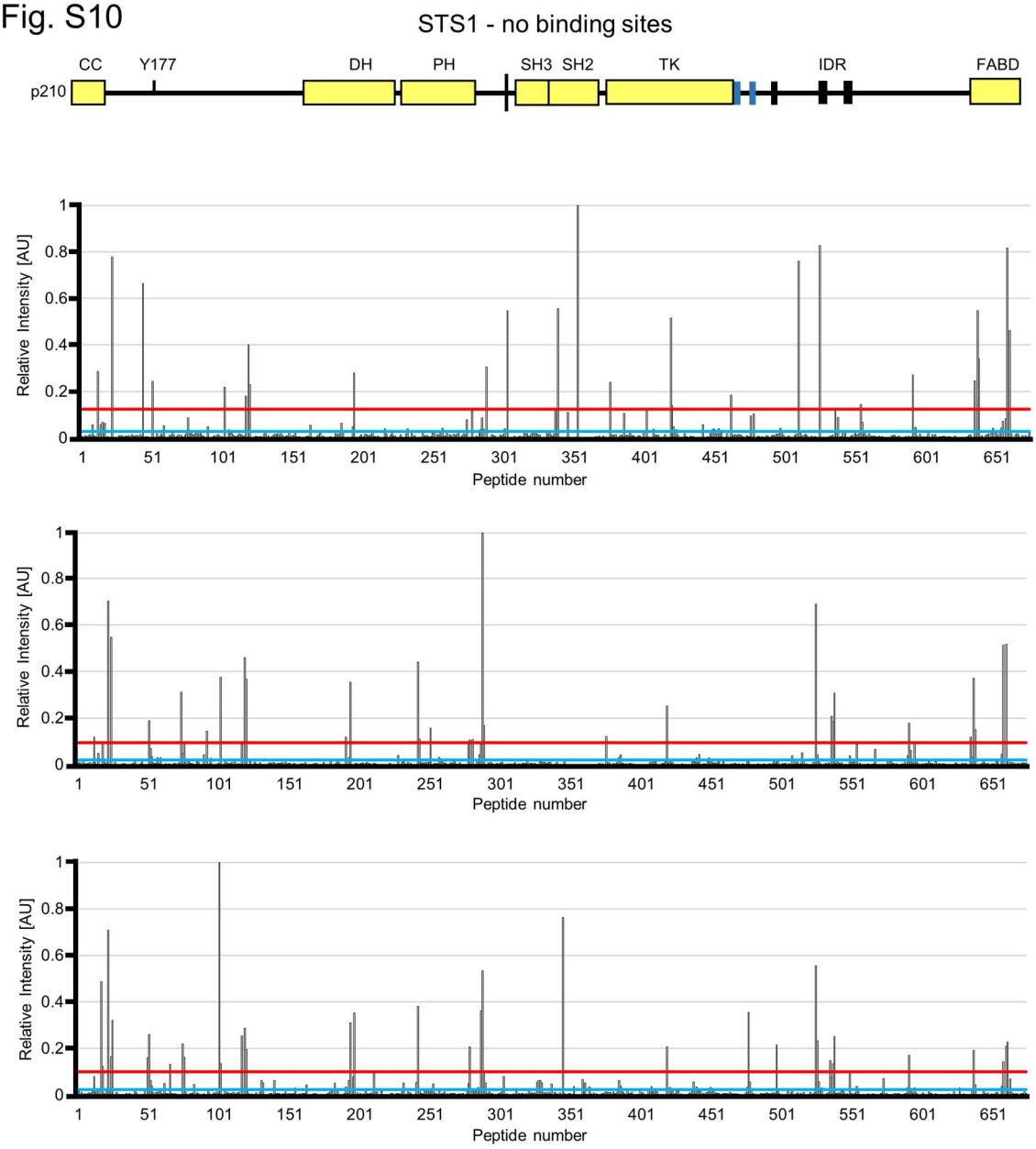


**Figure S10**
Microarray data for STS1 binding to BCR-ABL. No potential binding sites were detected.